

Supporting Information

Visible Photorelease of Liquid Biopsy Markers following Microfluidic Affinity-Enrichment

Thilanga N. Pahattuge,^{†[a]} J. Matt Jackson,^{†[a]} Digamber Rane,^[b] Harshani Wijerathne,^[a] Virginia Brown^[a],
Malgorzata A. Witek,^[a] Chamani Perera,^[b] Richard S. Givens,^[a] Blake R. Peterson,^[c] and Steven A.
Soper^{*[a,c,d,e]}

Experimental Methods

Reagents and materials. Microfluidic devices were fabricated using 6013S-04 cyclic olefin copolymer (COC) substrates and 5013S-04 COC coverslips (250 μm, TOPAS Advanced polymers). Microfluidic devices were connected to syringe pumps (New Era) using Inner-Lok™ union capillary connectors (Polymicro Technologies) and barbed socket Luer Lock™ fittings (3/32" ID, McMaster-Carr).

Reagents and materials included reagent-grade isopropyl alcohol (IPA), Micro 90®, 1-ethyl-3-[3-dimethylaminopropyl] carbodiimide hydrochloride (EDC), N-hydroxysuccinimide (NHS), anhydrous acetonitrile (ACN), anhydrous dimethylformamide (DMF), anhydrous dichloromethane (DCM), anhydrous triethyl amine (TEA), polyvinylpyrrolidone, 40 kDa (PVP-40), uranyl acetate (Sigma-Aldrich); toluidine blue O (TBO, Carolina Biological Supply); phosphate buffered saline (PBS, pH 7.4), sodium dodecyl sulfate (SDS, 10%), Hoechst 33342, SYTO® 82, LIVE/DEAD™ Cell Imaging Kit (Life Technologies); bovine serum albumin (BSA), acetic acid, hydrogen peroxide, sodium carbonate and bicarbonate, 2-(4-morpholino)-ethane sulfonic acid (MES), nuclease free water (Fisher Scientific); 10% (w/v) Tween-20, 10X Tris buffered saline (TBS), and SsoAdvanced™ Universal SYBR® Green Supermix (Bio-Rad); DNA Damage Competitive ELISA Kit (Invitrogen); 1 M Tris, pH 7.4 (KD Medical); Virkon S (Dupont); NEBuffer 2.1, Protoscript® II First Strand cDNA Synthesis Kit (New England Biolabs); phosphodiesterase I (Abnova); Novagen™ Benzonase® nuclease (EMD Millipore); FastAP Thermosensitive Alkaline Phosphatase (ThermoScientific); Cy5-oligonucleotide fluorescent reporter (5'-NH₂-C₁₂-

[a] T.N. Pahattuge, Dr. J.M. Jackson, H. Wijerathne, Dr. M.A. Witek, Prof. R.S. Givens, Prof. S.A. Soper
Center of BioModular Multi-Scale Systems
Department of Chemistry, University of Kansas
1140 ISB, 1567 Irving Hill Rd., Lawrence, KS 66045
E-mail: ssoper@ku.edu

† These authors contributed equally to this work.

[b] Dr. D. Rane, Dr. C. Perera, Prof. B.R. Peterson
Synthetic Chemical Biology Core Laboratory
Department of Medicinal Chemistry, University of Kansas
Structural Biology Center, 2034 Becker Dr., Lawrence, KS 66047

[c] V. Brown, Prof. S.A. Soper
Center of BioModular Multi-Scale Systems
Department of BioEngineering, University of Kansas
1132 Learned Hall, 1530 West 15th St., Lawrence, KS 66045

[d] Department of Mechanical Engineering
3138 Learned Hall, 1530 West 15th St., Lawrence, KS 66045

[e] Department of Cancer Biology and KU Cancer Center
University of Kansas Medical Center, Kansas City, KS

T₈CCCTTCCTCACTTCCCTTTUT₉-Cy5-3', HPLC-purified, Integrated DNA technologies); Direct-zol RNA and Quick-DNA purification kits (Zymo Research). All solvents were reagent grade.

Monoclonal antibodies (mAbs) were mouse anti-human Fibroblast Activation Protein, FAP α (clone 427819), mouse anti-human EpCAM/TROP-1 (clone 158210), mouse IgG2A isotype control (clone 133304), mouse anti-human CD8 α (clone 37006), Human EpCAM/TROP1 Alexa Fluor® 488-conjugated antibody (clone 158206), Human Fibroblast Activation Protein α /FAP Alexa Fluor® 488-conjugated antibody (clone 427819), Mouse IgG 2B Alexa Fluor® 488-conjugated Isotype control (clone 133303), Mouse IgG1 Alexa Fluor® 488-conjugated Isotype control (clone 11711) all from R&D Systems. Cell lines were purchased from the American Type Culture Collection (ATCC). Culture reagents included fetal bovine serum (FBS, Performance, Gibco), McCoy's 5A (Corning), high glucose HyClone™ DMEM (GE Life Sciences), RPMI-1640 (ATCC), recombinant bovine insulin (Sigma), TrypLE express reagent (Thermo Fisher), and 25 cm² tissue culture flasks (Fisher Scientific). TEM grids (Carbon type B, 300 mesh) were purchased from Ted Pella Inc. Blocking and washing buffers were filtered (0.2 μ m, PTFE, Fisher Scientific) just prior to use. Nuclease-free microfuge tubes (Fisher Scientific) were used for preparation and storage of all samples and reagents.

Surface characterization of UV/O₃-activated COC exposed to organic solvents. COC plates (6013S-04) were diced into 1" square pieces, cleaned by rinsing with 10% Micro-90, IPA, and nanopure water, and dried at 60°C for >1 h. Substrates were UV/O₃-activated (16.1 min, 22 mW/cm² measured at 254 nm)¹ and either left in air or immersed in 100 mM MES buffer (pH = 4.8) or anhydrous solvents – ACN, DMF, or DCM – for 2 h. Treated substrates were rinsed with copious amounts of nanopure water and dried with N₂ before analysis. Water contact angles (WCAs) were measured by dispensing 2.0 μ L of nanopure water onto the substrate using a VCA Optima instrument (AST Products). Three measurements were averaged per substrate.

Carboxylic acid (-COOH) surface densities were measured via toluidine blue O (TBO). The TBO assay¹ was performed using an *in situ* incubation chamber (Bio-Rad) and placing the chamber on substrate and covering the surface with 0.1% (w/v) TBO in 50 mM carbonate buffer (pH = 10.5). After 15 min, the substrate was submerged in the same buffer for 15 min then N₂-dried. TBO was desorbed using 40% acetic acid (d = 1.0196 g/mL) and collected in a pre-weighed microfuge tube. TBO concentrations were determined with either a Shimadzu UV-1280 UV/Vis spectrophotometer or a BioTek Synergy H4 Hybrid plate reader against a calibration curve and a 40% acetic acid blank.

Attenuated total reflectance Fourier transform infrared (ATR-FTIR) spectra were secured using a Shimadzu IRAffinity-1S equipped with a Specac Quest ZnSe ATR accessory. Each scan (340-4700 cm⁻¹) was averaged 45 times and processed by a 3-point baseline correction (1500, 2000, and 4000 cm⁻¹) before integrating peak areas for carbonyls (1650-1850 cm⁻¹) and hydroxyls (3200-3700 cm⁻¹).

Fabrication of microfluidic devices. The microfluidic device used for CTC affinity-enrichment consisted of 50 sinusoidal high aspect ratio microchannels (25 μ m \times 150 μ m, w \times h) interconnected in a Z-configuration.¹⁻⁹ EV

affinity-enrichment used a microfluidic device with three, serially-connected beds populated with a total of 15,202 micropillars (110-120 μm pillar diameter, 10-20 μm pillar spacing).¹⁰

Mold masters were prepared in brass using high precision-micromilling (KERN 44, KERN Micro- und Feinwerktechnik GmbH & Co.KG; Murnau, Germany) with carbide bits (Performance Micro Tool). COC devices were fabricated from the brass mold masters by hot embossing.^{6, 10} Hot embossing of the CTC affinity-enrichment device was performed at 155°C and 30 kN force for 120 s using a HEX03 embossing machine (Jenoptik Optical systems GmbH), and for EV affinity-enrichment device, devices were embossed at 162°C with 900 lb force using a precision press (Wabash MPI) followed by manual cooling and demolding at 150°C. Mold release agent (MoldWiz® F57-NC) was kindly gifted by Axel Plastics.

Measurements of the mold and replicated devices were made with a VK-X 3D laser scanning confocal microscope (Keyence). Embossed devices were taped, diced with a bandsaw, immediately cleaned of debris by sonicating in 10% Micro-90 and rinsing with IPA and nanopure water, and finally dried at 60°C for ≥ 30 min. COC cover plates (250 μm thickness) were cut, rinsed with 10% Micro-90, IPA, and nanopure water, and similarly dried. Cleaned devices and 250 μm COC cover plates were UV/O₃-activated (15 min, 27 mW/cm² measured at 254 nm) in a Model 18 UVO-Cleaner® (Jelight Company).^{11, 12} Devices were fitted with glass capillaries (365 μm OD, 150 μm ID) and an inverted UV/O₃-activated cover plate, and clamped between two glass plates for thermal fusion bonding (134°C, 1 h). Capillary fittings were sealed with epoxy after annealing.

Immobilization of Cy5 oligonucleotide fluorescent reporter. Flat substrates or thermal fusion bonded microfluidic devices were UV/O₃-activated and/or treated with solvents as described above. Surfaces or devices were then reacted with EDC (20 mg/mL) and NHS (2 mg/mL), either solubilized in 100 mM MES buffer (pH = 4.8) by pipetting or in anhydrous ACN by vigorous vortexing, for 25 min at room temperature. After air-drying, ssDNA oligonucleotides with 5'-NH₂, 3'-Cy5 functionalities were infused at 10-40 μM concentration in PBS. The reaction was carried out for 2 h at room temperature before rinsing with ~ 1 mL 0.1% SDS and finally PBS. Flat substrates were dried before imaging and sealed with tape. Imaging was conducted with a Zeiss Axiovert 200M microscope using a 10X objective (0.3 NA, Plan NeoFluar), an XBO 75 W lamp, Cy5 filter set (Omega Optical), a Cascade 1K EMCCD camera (Photometrics), and a MAC 5000 stage (Ludl Electronic Products), all of which were computer-controlled via Micro-Manager. Images were background subtracted, measured, and intensity-scaled for display in ImageJ.

PC linker synthesis and characterization. Synthetic procedures for the PC linker are described in detail below. All reactions were performed under an inert atmosphere of dry argon or nitrogen, and used either flame-dried or oven-dried glassware or in a glass microwave vial (Biotage, LLC). All anhydrous solvents were purchased from Sigma Aldrich and dried via passage through a glass contour solvent system (Pure Process Technology, LLC). Thin-layer chromatography (TLC) was performed using commercial aluminum backed silica plates (TLC Silica gel 60 F254, Analytical Chromatography), and plates were visualized by UV irradiation. Flash chromatography

used a normal-phase silica gel (230–400 mesh), normal-phase Combiflash purification system (gold silica column), or reverse-phase Combiflash purification system (50 g HP C18 gold column).

Nuclear magnetic resonance (NMR) spectra were recorded on either a 400 MHz or 500 MHz Bruker Avance spectrometer with a dual carbon/proton cryoprobe. NMRs were recorded in deuterated chloroform or methanol. Chemical shifts are reported in parts per million (ppm) and referenced to the center line of the solvent (δ 3.31 and 7.26 with respect to methanol- d_4 and chloroform- d for ^1H NMR, and δ 49.00 and 77.16 with respect to methanol- d_6 and chloroform- d for ^{13}C NMR). Coupling constants are given in Hertz (Hz). The spin multiplicities are reported as s = singlet, d = doublet, t = triplet, q = quartet, dd = doublet of doublet, td = doublet of triplet, and m = multiplet. NMR data was analyzed using MestReNova 14 software. High-resolution mass spectrometry (HRMS) data were collected on an LCT Premier (Waters Corporation) time-of-flight mass spectrometer.

The synthesized PC linker was dissolved in 1x PBS (2.1 μM) and exposed to visible light (400–450 nm, 34 ± 4 mW/cm 2). Samples (50 μL) were withdrawn after 1 min, 2 min and 10 min light irradiation and analyzed by UPLC/HRMS (Waters Acquity UPLC with a photodiode array UV detector and an LCT Premiere TOF mass spectrometer). The gradient mobile phase consisted of water/acetonitrile (95:5 to 0:100 containing 0.05% TFA) over 2.7 min. The column was a Waters Acquity Atlantis T3 2.1x 50 mm, 1.7 μm column operated at a flow rate of 0.6 mL/min. The wavelength of detection was 247 nm and the volume injected onto the column was 2 μL .

Immobilization of PC linker, Cy5 fluorescent reporters, or mAbs. Devices were UV/O $_3$ -activated then thermal fusion bonded to cover plates as described above. EDC (20 mg/mL) and NHS (2 mg/mL) were dissolved in dry ACN and infused into the device using all-plastic, Norm-JectTM syringes (Air-Tite). Next, devices were wrapped in a protective Rubylith[®] film (Ulano) to prevent subsequent exposure of the PC linker to ambient light. After 25 min incubation at room temperature, reagents were displaced by air, and the PC linker (dissolved in dry ACN with a 2 molar excess of TEA) was infused into the device via a vacuum pump. After incubating 2 h at room temperature, reagents were displaced by air, and the device was infused with 100 mM Tris (pH 7.4) and incubated for 30 min at room temperature to inactivate any unreacted NHS ester groups on the device's surface. A second EDC/NHS reaction in dry ACN, as described above, was performed to activate the -COOH group at the end of the PC linker. Either Cy5 oligonucleotide reporters (40 μM) dissolved in PBS (pH 7.4) or mAbs (1 mg/mL) were incubated for 2 h at room temperature or overnight at 4°C, respectively. For Cy5 reporters, the device was washed with 0.1% SDS and finally PBS. When changing between anhydrous solvents and any buffered solution, devices were briefly flushed with nuclease free water (10–30 μL), then excess solvent or buffer as a preventative measure against salt precipitation.

LED light exposure system and monitoring PC linker cleavage via Cy5 reporters. An 885 mW LED (M420L3, ThorLabs) producing light from 385–470 nm ($\lambda_{\text{max}} = 412$ nm) was filtered through a 400 nm longpass colored glass filter (Edmund Optics) that was used to photocleave the PC linker. The LED's innate divergence (60°) illuminated a 90 mm diameter spot at 24 mm distance. The power distribution was measured with an 18 mm x 18 mm power sensor (ThorLabs) rastered beneath the LED spot. These measurements were then fit with

a 2D Gaussian and integrated over the device's surface area in Matlab. For photocleavage reactions, the LED was mounted to a polished aluminum chamber with recesses that centered devices 24 mm beneath the LED, and the LED was triggered using an analog LED driver (Thorlabs) and a custom electronic timer.

For releasing Cy5 reporters immobilized via the PC linker, devices were first imaged by fluorescence microscopy as described above. Devices were then exposed to LED light for 1 min. Released Cy5 reporters were removed from the device by infusing PBS, collected into a pre-weighed microcentrifuge tube, and quantified against a calibration curve by fluorometry (Jobin-Yvon Fluorolog 3, $\lambda_{\text{ex}} = 642 \text{ nm}$, $\lambda_{\text{em}} = 664 \text{ nm}$). Devices were imaged by microscopy again after the photocleavage process was repeated for an additional 1 min (2 min total exposure) and a final 8 min LED exposure (10 min total) to investigate the efficiency of photocleavage as a function of dose.

Cell culture, analysis of cellular antigen expression, cell enrichment, and release. SKBR3, MCF7, and Hs578T (breast cancer) cell lines were cultured at 37°C under a 5% CO₂ atmosphere in 1x McCoy's 5A/10% FBS, 1x MEM alpha/10% FBS and 1.7 μM human insulin, or DMEM/10% FBS/ and 1.7 μM bovine insulin, respectively. Cells were harvested for experiments using TrypLE express reagent (5 min), centrifuged (300 g, 10 min), and resuspended in ice cold PBS.

For the analysis of cell line antigen expression levels, harvested cells were washed with ice cold PBS (three times) and fluorescently labeled primary antibody (Alexa Fluor 488, h-EpCAM or h-FAP α) was added to the cells (5-10 $\mu\text{l}/10^6$ cells in suspension). The suspension was mixed well and allowed to incubate for 30 min at room temperature in the dark. Next, the cells were washed with 0.1% BSA (in PBS) three times to remove any unbound conjugated antibodies. After the final washing step, cells were resuspended in ice cold PBS, filtered (0.2 μm , PTFE), and analyzed by flow cytometer (BD Accuri C6). Results were compared with a suitable isotype control (Alexa Fluor 488, IgG 2B or IgG1).

De-identified blood samples from healthy donors were provided by the KU Cancer Center's Biospecimen Repository Core Facility (BRCF) under the repository's IRB approved protocol (HSC #5929). Peripheral blood samples were drawn into Vacuette® K3EDTA (Greiner) tubes under the IRB-approved KUMC Biorepository protocol.

Prior to sample infusion, CTC devices modified with the PC linker and anti-EpCAM mAbs were infused with 2 mL of 0.5% BSA/PBS at 50 $\mu\text{L}/\text{min}$ to remove unbound mAbs and block the surface to minimize nonspecific adsorption. SKBR3 cells were pre-stained with Hoechst 33342 (40 $\mu\text{g}/\text{mL}$, 15 min, RT), resuspended in PBS, then spiked into a 1 mL blood sample (69-269 SKBR3 cells/mL). The spiked blood was loaded into a 1-3 mL syringe (BD) and hydrodynamically infused through two devices in series at a flow rate of 25 $\mu\text{L}/\text{min}$ (2 mm/s linear velocity). After blood processing, nonspecifically bound cells were removed by rinsing with 1 mL of 0.5% BSA/PBS at a flow rate of 50 $\mu\text{L}/\text{min}$ (4 mm/s linear velocity). All captured cells were stained with SYTO 82 nucleic acid dye (5 μM , infused at 25 $\mu\text{L}/\text{min}$ and incubated for 15 min). Excess dye was removed with 0.5% BSA/PBS (50 $\mu\text{L}/\text{min}$, 100 μL). Devices were exposed to the LED system (2 min, $32 \pm 4 \text{ mW cm}^{-2}$, described above), and released cells rinsed with 0.5% BSA/PBS (50 $\mu\text{L}/\text{min}$, 250 μL) and collected into a flat bottom 96-

well plate for fluorescence microscopy (DAPI and Cy3 filters). Additionally, the microfluidic device was manually scanned to enumerate cells that were not released.

SKBR3 cells were identified as positive for both Hoechst 33342 and SYTO 82, whereas nonspecific leukocytes were positive for SYTO 82 only. Purity was calculated as the ratio of SKBR3 cells to total cell count (SKBR3 cells + leukocytes). Release efficiency was calculated as the ratio of released cells to the total cell count (released cells + cells on-chip). Capture efficiency was determined by self-referencing, where the SKBR3 cells captured in the first device was divided by the total cell count (first device + second device).^{9, 13} Mouse IgG2A isotype control mAb was immobilized through the PC linker to evaluate nonspecifically bound SKBR3 cells. This was undertaken to gauge the release efficiency of MCF7 and Hs578T cells spiked into PBS buffer using Hoechst 33342 staining only. In the case of Hs578T cell experiments, anti-FAP α mAbs were used.

The effect of PC release on cell viability, cultivation, and oxidative DNA/RNA damage. SKBR3 cells were spiked into PBS and affinity-enriched with anti-EpCAM mAbs. Cells were released by 2 min LED exposure, collected into a 96-well plate, and stained for viability using calcein AM and ethidium homodimer I (LIVE/DEAD Cell Imaging Kit) for 15 min at room temperature. The plate was centrifuged (300 rcf, 5 min), and staining reagents were aspirated and replaced with PBS for fluorescence microscopy. Viability measurements were taken from ~100 released cells (for other cell lines, the release step was omitted, and cells were directly exposed in a 96-well plate – for these viability measurements, several thousand cells were averaged). For monitoring cell cultivation after release, SKBR3 cells (180 cells) were seeded into the experiment and were then cultured (as described above) for up to 4 d.

LED-induced DNA/RNA damage was determined by measuring the oxidative product of DNA/RNA, 8-oxo guanine (8-oxo-G).^{14, 15} Hs578T cells were grown in 35 mm diameter tissue culture dishes (Fisher Scientific) until ~80% confluency. The cells were washed with ice cold PBS, covered with 1 mL ice cold PBS, and the culture dish was irradiated in an ice bath in the LED exposure system for 2 min (18.47 J). In a control experiment, the cells were placed in the exposure system for 2 min without irradiation. To allow for comparison of LED exposure and UV exposure, this process was repeated with an equivalent dosage of UV light (18.47 J) using a UVP CL-1000 crosslinker chamber (Analytik Jena). Results from UV and LED irradiation were compared to results obtained from H₂O₂ treated cells. Briefly, the cells were washed twice with ice cold PBS, incubated in 10 mL H₂O₂ (300 μ M in 1X PBS) for 30 min at 37°C and 5% CO₂, then washed twice with ice cold PBS.

DNA or RNA was immediately extracted following irradiation using Zymo Quick-DNA and Direct-zol RNA isolation kits according to the manufacturer's protocol. Extracted DNA/RNA was quantified by UV-Vis (Shimadzu BioSpec-nano) and High Sensitivity RNA or Genomic DNA TapeStation (Agilent) and diluted to 80 ng/ μ L, and 6 μ g substrate was digested into mononucleotides using 18 mU phosphodiesterase I, 15 U benzonase nuclease, and 12 U alkaline phosphatase¹⁶ in NEBuffer 2.1. 8-oxoG quantification was performed in triplicate using a DNA Damage Competitive ELISA Kit (Invitrogen) according to the manufacturer's protocol.

To establish the impact of RNA oxidative damage on the ability to conduct mRNA profiling, 1 μg non-digested RNA was reverse-transcribed into cDNA using Protoscript® II and poly(dT) primers at 42°C for 1 h followed by enzyme deactivation at 80°C for 5 min. cDNA was diluted 5-20 \times before being amplified by qPCR with gene-specific primers (200 nM for all genes except 125 nM for *MMP9*, **Table S2**), SsoAdvanced™ SYBR Green master mix, and a CFX Connect Real-Time System (BioRad). The PCR thermocycling protocol was 95°C for 5 min and 40 cycles of 95°C for 30 s, 50°C for 30 s, and 72°C for 1 min.

The effect of attached Ab ligands on cell mRNA expression. RT-qPCR was performed to investigate the molecular level changes caused by the photorelease assay and antibodies remaining on the cell surface following photorelease. For these tests, the PC linker and anti-EpCAM Abs were immobilized onto UV/O₃-COC treated surfaces and cells were enriched from the blood samples using the antibody-decorated chip. Devices were washed with 0.5%BSA/PBS (50 $\mu\text{L}/\text{min}$, 250 μL) and exposed to 2 min of LED blue light. Photoreleased cells were lysed, total RNA was extracted, and quantified (the time between the cell affinity selection and cell lysis was \sim 1 h). Complementary DNA (cDNA) was synthesized by performing reverse transcription (RT) with the Protoscript® II cDNA synthesis Kit and anchored d(T)₂₃ VN primers (**Table S2** for primer sequences) according to New England Biolabs' protocol. RT-qPCR was performed as described above. SKBR3 cells taken from culture were used as the control.

Anti-CD8 enrichment of MOLT-3-derived EVs. MOLT-3 cells were cultured at 37°C and 5% CO₂ in RPMI-1640 with 10% FBS. FBS was depleted of background bovine EVs via ultracentrifugation (100,000 rcf, 18 h, 4°C) with an L8-80M ultracentrifuge, Type 45 Ti rotor, 38 mm \times 102 mm (70 mL) polycarbonate tubes (Beckman Coulter), and a mechanical Harvard Trip balance (OHAUS). Tubes were sterilized with 10% hydrogen peroxide before use and disinfected with Virkon S when transferring between the centrifuge and culture hood. After ultracentrifugation, the FBS supernatant was decanted, mixed thoroughly to homogenize protein content, aliquoted, and stored at -20°C. Cells were transitioned into EV-depleted FBS for 1 week before obtaining MOLT-3 conditioned media by centrifugation (2000 \times g, 10 min).

EV microfluidic affinity-purification devices were modified with the PC linker and a monoclonal anti-CD8 Ab as described above. Before affinity-enrichment, EV microfluidic devices were washed with 400 μL blocking buffer (1% BSA, 1% PVP-40 in PBS) at 10 $\mu\text{L}/\text{min}$. Conditioned media (500 μL) was infused at 5 $\mu\text{L}/\text{min}$, then the device was washed with 400 μL 0.2% Tween 20 in TBS buffer and then 50 μL PBS at 10 $\mu\text{L}/\text{min}$. After LED exposure, released EVs were collected in 400 μL PBS (20 $\mu\text{L}/\text{min}$) and stored at -80°C for subsequent analysis.

Nanoparticle tracking analysis (NTA). Thawed samples were heavily vortexed, loaded into a 1 mL syringe (BD), and infused into the flow cell of a NanoSight LM10 NTA instrument (Malvern Panalytical) equipped with a 488 nm laser and NTA 2.3 software. In some cases, samples were diluted to ensure 10-100 EVs per frame. Imaging used a camera shutter setting of 1206, camera gain of 366, 90-160 s acquisition times, and 5 averaged replicates where the sample was advanced by \sim 25 μL while the camera was off to image a random portion of the sample for each replicate. Processing used the Detection Threshold 20 and all other automatic settings. Between each sample, the flow cell was slowly flushed with 1 mL PBS then air four times, and flushing was verified by manually monitoring the number of nanoparticles observed in 300 μL PBS (\sim 0-1 per 100 μL).

Nanoparticle concentrates were multiplied by each assay's elution volume to report the number of nanoparticles released.

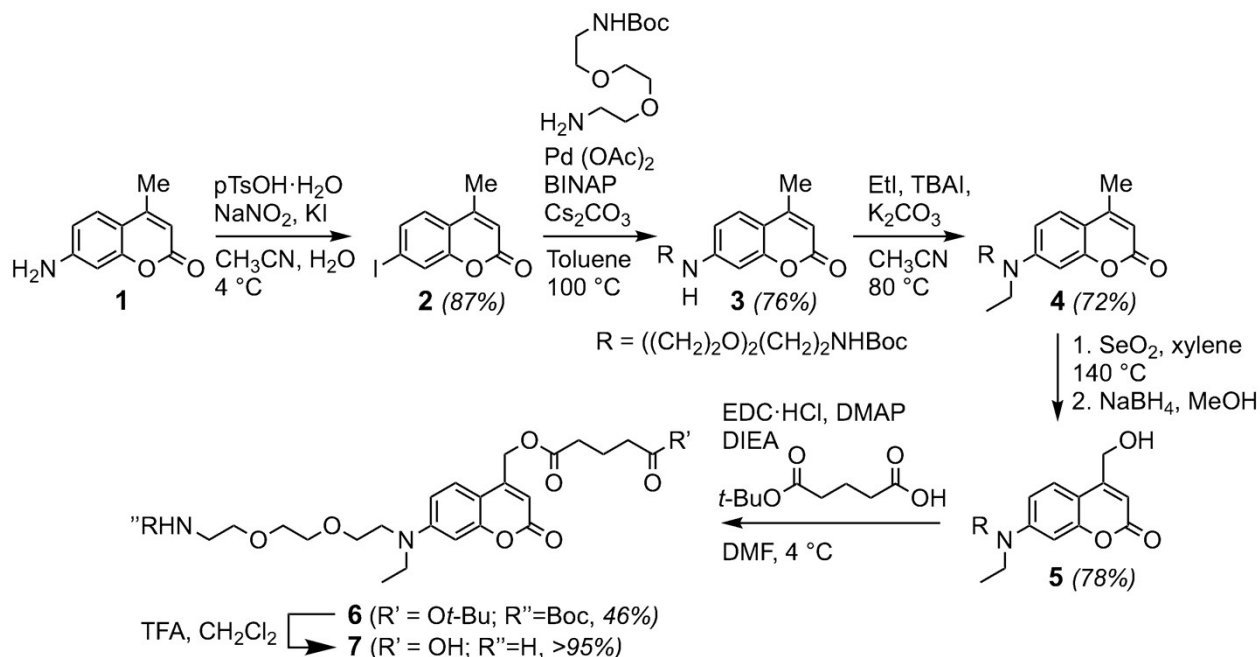
Transmission electron microscopy (TEM) imaging. Samples were heavily vortexed and spotted onto TEM grids. After 20 min, excess buffer was blot dried, and the grids were washed three times with a drop of nanopure water for 10 s. Grids were blot dried and stained with 5 μ L 2% (w/v) uranyl acetate (0.22 μ m filtered) for 10 s. Grids were blot dried, air dried for 15 min, and imaged with a Technai F20 XT Field Emission TEM (FEI).

LED-induced mRNA damage of EVs. A panel of genes (*MMP9*, *PLBD1*, *FOS*, *CA4* and *VCAN*) was previously identified for diagnosing acute ischemic stroke (AIS).¹⁷ We used this gene panel to determine if there was LED-induced damage of EV mRNA that may affect their expression profiles. MOLT-3 conditioned media was obtained from culture as described above. Cells were removed by centrifugation (300 rcf for 10 min), and EVs were precipitated using the ExtraPEG procedure.¹⁸ To 3 mL conditioned media, we spiked an equal volume of PEG and NaCl (final concentration of 12% and 0.5 M, respectively), mixed by pipetting, incubated overnight at 4°C, centrifuged the sample (4000 rcf for 1 h), removed the supernatant, washed the pellet with ice cold PBS, resuspended the pellet in PBS (6 mL) by pipetting and vortexing, and aliquoted 1 mL portions into 35 mm diameter tissue culture dishes. Culture dishes were placed in an ice bath, inserted in the LED chamber, and either not exposed (control) or exposed for 2 min (18.5 J) by the LED. The EV suspension was then removed from the culture dish, and 1 mL of TRI Reagent was added to lyse EVs. The RNA was extracted using Direct-zol RNA extraction kit according to Zymo's guidelines and analyzed with a 2200 TapeStation and High Sensitivity RNA reagents (Agilent).

Reverse transcription and droplet digital PCR (RT-ddPCR). Complementary DNA (cDNA) was synthesized by performing RT with the Protoscript® II cDNA synthesis Kit and anchored d(T)₂₃ VN primers according to New England Biolabs' protocol. cDNA product was used to generate droplets with the QX200 droplet generator, EvaGreen® Supermix, and gene specific primers (**Table S3**, 125 nM) followed by PCR amplification with the BioRad C1000 thermal cycler and the above thermocycling protocol. Final cooling was carried out at 4°C. Droplets were read with a BioRad QX200 droplet reader, and data analyzed using QuantaSoft™ software. All data were normalized to the total RNA concentration.

Supplementary Results

Synthetic procedures and compound characterization for PC linker. 7-iodo-4-methyl-2H-chromen-2-one (2): As shown in **Scheme S1**, 7-iodo-4-methyl-2H-chromen-2-one was prepared using a previously described procedure.¹⁹ Briefly, 7-amino-4-methyl-2H-chromen-2-one **1** (710 mg, 2.48 mmol, 1 equiv.), and *p*-toluenesulfonic acid monohydrate (1.63 g, 8.56 mmol, 3.0 equiv.) were weighed in a single necked round bottom flask (100 mL) and suspended in acetonitrile:water (6 mL, 1:1). The suspension was cooled to 4°C for 5 min and treated dropwise with sodium nitrite (390 mg, 5.70 mmol, 2.0 equiv.) and potassium iodide (1.18 g, 7.13 mmol, 2.5 equiv.) in water (4 mL). Vigorous effervescence was observed. After the addition of this reagent was complete, the reaction mixture was stirred at 4°C for an additional 10 min and then stirred at room temperature (23°C) for 3-4 h. Reaction progress was monitored by TLC and upon completion, saturated aqueous sodium bicarbonate was added to adjust the pH to 9. The reaction mixture was then diluted with ethyl acetate (~250 mL), and the organic layer was extracted with water (2 x 50 mL) and saturated aqueous sodium thiosulfate (50 mL). The organic layer was dried over anhydrous sodium sulfate, filtered, and concentrated to dryness. The residue was re-dissolved in dichloromethane and purified by silica gel chromatography using hexane and ethyl acetate to elute **2** (710 mg, 87% yield) as a colorless solid. ¹H NMR (400 MHz, Chloroform-*d*) δ 7.73 – 7.69 (m, 1H), 7.65 – 7.60 (m, 1H), 7.30 (d, *J* = 8.3 Hz, 1H), 6.31 (d, *J* = 1.5 Hz, 1H), 2.42 (d, *J* = 1.2 Hz, 3H); ¹³C NMR (101 MHz, Chloroform-*d*) δ 160.0, 153.6, 152.0, 133.6, 126.3, 125.7, 119.7, 115.8, 97.3, 18.7.



Scheme S1. Synthesis of 5-((7-((2-(2-(2-aminoethoxy)ethoxy)ethyl)(ethyl)amino)-2-oxo-2H-chromen-4-yl)methoxy)-5-oxopentanoic acid (**7**).

tert-butyl(2-(2-(2-((4-methyl-2-oxo-2H-chromen-7-yl)amino)ethoxy)ethoxy)ethyl)carbamate (3): As shown in **Scheme S1**, the iodide **2** (120 mg, 0.42 mmol, 1.0 equiv.), amine (124 mg, 0.5 mmol, 1.2 equiv.), Pd(OAc)₂ (9.5

mg, 0.042 mmol, 0.1 equiv.), Xantphos (36.4 mg, 0.063 mmol, 0.15 equiv.) and Cs₂CO₃ (342 mg, 1.05, 2.5 equiv.) were weighed in a Biotage microwave reaction vial in a glove box. The mixture was treated with toluene (6 mL), and the vial was sealed and removed from the glove box. The reaction mixture was heated in an oil bath at 100 °C for 6 h. The crude mixture was then cooled to room temperature and purified by silica gel chromatography using hexane and ethyl acetate to elute **3** (129 mg, 76% yield) as a viscous oil. ¹H NMR (400 MHz, Chloroform-*d*) δ 7.36 (d, *J* = 8.6 Hz, 1H), 6.59 (s, 1H), 6.50 (s, 1H), 5.99 (s, 1H), 4.99 (s, 1H), 3.73 (t, *J* = 5.1 Hz, 2H), 3.65 (s, 4H), 3.56 (t, *J* = 5.2 Hz, 2H), 3.38 (t, *J* = 5.1 Hz, 2H), 3.33 (s, 2H), 2.34 (d, *J* = 1.0 Hz, 3H), 1.44 (s, 9H); ¹³C NMR (101 MHz, CDCl₃) δ 162.0, 156.1, 156.1, 153.1, 151.5, 125.6, 110.9, 110.8, 109.6, 98.3, 79.5, 70.5, 70.3, 70.3, 69.2, 43.2, 40.5, 28.5, 18.6; HRMS calcd. for C₂₁H₃₁N₂O₆⁺: 407.2182; Found: 407.2187.

tert-butyl(2-(2-(2-(ethyl(4-methyl-2-oxo-2*H*-chromen-7-yl)amino)ethoxy)ethoxy)ethyl)carbamate (**4**): As shown in **Scheme S1**, the amine **3** (35 mg, 0.086 mmol, 1.0 equiv.), tetrabutylammonium iodide (31.7 mg, 0.086 mmol, 1.0 equiv.) and potassium carbonate (41.5 mg, 0.30 mmol, 3.5 equiv.) were weighed in a flame-dried, Ar-flushed Biotage microwave reaction vial. The mixture was treated with anhydrous acetonitrile (3 mL) and iodoethane (0.027 mL, 0.344 mmol, 4.0 equiv.). The vial was sealed and heated in an oil bath at 80 °C for 16 h. After 16 h, the reaction mixture was treated with additional 2.0 equiv. of iodoethane and heated for 18-20 h. Progress of the reaction was monitored by TLC, and upon completion, the reaction was diluted with ethyl acetate (25 mL) and transferred to a separatory funnel. The organic layer was washed with water (2 x 10 mL), dried over sodium sulfate, and concentrated to dryness. The residue was re-dissolved in dichloromethane and purified by silica gel chromatography using hexane and ethyl acetate to elute **4** (27 mg, 72% yield) as a viscous oil. ¹H NMR (400 MHz, Chloroform-*d*) δ 7.39 (d, *J* = 8.9 Hz, 1H), 6.67 (dd, *J* = 8.9, 2.2 Hz, 1H), 6.56 (d, *J* = 2.3 Hz, 1H), 5.97 (d, *J* = 1.0 Hz, 1H), 4.96 (s, 1H), 3.69 – 3.64 (m, 2H), 3.62 – 3.55 (m, 6H), 3.53 (t, *J* = 5.2 Hz, 2H), 3.48 (q, *J* = 7.1 Hz, 2H), 3.30 (s, 2H), 2.34 (d, *J* = 1.0 Hz, 3H), 1.44 (s, 9H), 1.20 (t, *J* = 7.1 Hz, 3H); ¹³C NMR (101 MHz, CDCl₃) δ 162.2, 156.1, 156.0, 152.9, 150.7, 125.6, 109.9, 109.4, 108.9, 98.4, 79.4, 70.9, 70.4, 70.4, 68.7, 50.5, 46.2, 40.5, 28.6, 18.6, 12.1; HRMS calcd. for C₂₃H₃₅N₂O₆⁺: 435.2495; Found: 435.2487.

tert-butyl(2-(2-(2-(ethyl(4-(hydroxymethyl)-2-oxo-2*H*-chromen-7-yl)amino)ethoxy)ethoxy)ethyl) carbamate (**5**). As shown in **Scheme S1**, **4** (54 mg, 0.12 mmol, 1.0 equiv.) and selenium dioxide (27.5 mg, 0.24 mmol, 2.0 equiv.) were weighed in a flame-dried, Ar-flushed, single-necked round bottom flask (25 mL) equipped with a water-cooled condenser. The mixture was treated with *p*-xylene (5 mL) and heated in an oil bath at 140°C for 24 h. The crude reaction mixture was cooled to room temperature and concentrated to dryness. Formation of the intermediate aldehyde was verified by ¹H NMR in chloroform-*d*. The crude mixture was then re-dissolved in methanol (1 mL), treated with sodium borohydride (14.0 mL, 0.37 mmol, 3.0 equiv.), and stirred at room temperature (23 °C) for 3 h. The progress of the reaction was monitored by TLC, and upon completion, the reaction mixture was concentrated to dryness. The crude mixture was re-dissolved in dichloromethane and purified by silica gel chromatography using hexane and ethyl acetate to elute **5** (44 mg, 78% yield) as a viscous oil. ¹H NMR (400 MHz, Chloroform-*d*) δ 7.31 (d, *J* = 9.0 Hz, 1H), 6.60 (dd, *J* = 9.0, 2.5 Hz, 1H), 6.52 (d, *J* = 2.5 Hz, 1H), 6.27 (s, 1H), 5.00 (s, 1H), 4.80 (s, 2H), 3.64 (t, *J* = 5.8 Hz, 2H), 3.57 (d, *J* = 13.2 Hz, 6H), 3.52 – 3.42

(m, 4H), 3.27 (q, $J = 5.0$ Hz, 2H), 1.42 (s, 9H), 1.18 (t, $J = 7.1$ Hz, 3H); ^{13}C NMR (101 MHz, CDCl_3) δ 162.6, 156.2, 156.1, 155.0, 150.7, 124.6, 109.0, 107.0, 106.1, 98.3, 79.5, 70.9, 70.4 (2 overlapping carbons), 68.7, 61.0, 50.3, 46.0, 40.4, 28.5, 12.1; HRMS calcd. for $\text{C}_{23}\text{H}_{35}\text{N}_2\text{O}_7^+$: 451.2444; Found: 451.2455.

tert-butyl ((7-((2,2-dimethyl-4-oxo-3,8,11-trioxa-5-azatriodecan-13-yl)(ethyl)amino)-2-oxo-2*H*-chromen-4-yl)methyl) glutarate (6). As shown in **Scheme S1**, 5-*(tert*-butoxy)-5-oxopentanoic acid (20 mg, 107 μmol , 1.1 equiv.), EDC·HCl (22.5 mg, 117 μmol , 1.2 equiv.) and dimethylaminopyridine (1.2 mg, 9.7 μmol , 0.1 equiv.) were weighed in a flame-dried, Ar-flushed microwave vial. The mixture was cooled to 0 °C and sequentially treated with anhydrous DMF (0.5 mL) and DIEA (35 μL , 195 μmol , 2.0 equiv.) and stirred for 30 min. The reaction mixture was then treated dropwise with alcohol **5** (44 mg, 97 μmol , 1.0 equiv.) as a solution in DMF (1.0 mL). The reaction mixture was stirred at 0 °C for 10 min and then warmed to room temperature (23 °C). The reaction mixture was stirred for an additional 16-18 h. Upon completion, the reaction mixture was diluted with ethyl acetate (25 mL) and transferred to a separatory funnel. The organic layer was washed with water (2 x 10 mL), dried over sodium sulfate, and concentrated to dryness. The residue was re-dissolved in dichloromethane and purified by silica gel chromatography using hexane and ethyl acetate to elute **6** (28 mg, 46% yield) as a viscous oil. ^1H NMR (600 MHz, Chloroform- d) δ 7.29 (d, $J = 9.0$ Hz, 1H), 6.61 (dd, $J = 9.0, 2.6$ Hz, 1H), 6.55 (d, $J = 2.5$ Hz, 1H), 6.14 (s, 1H), 5.22 (d, $J = 1.4$ Hz, 2H), 4.94 (s, 1H), 3.66 (t, $J = 6.0$ Hz, 2H), 3.59 (d, $J = 17.0$ Hz, 6H), 3.53 (t, $J = 5.3$ Hz, 2H), 3.48 (q, $J = 7.1$ Hz, 2H), 3.31 (q, $J = 5.5$ Hz, 2H), 2.50 (t, $J = 7.5$ Hz, 2H), 2.31 (t, $J = 7.3$ Hz, 2H), 1.97 (m, 2H), 1.44 (d, $J = 4.4$ Hz, 18H), 1.20 (t, $J = 7.0$ Hz, 3H); ^{13}C NMR (151 MHz, Chloroform- d) δ 172.5, 172.2, 161.9, 156.3, 156.1, 151.0, 149.5, 124.5, 109.0, 107.0, 106.5, 98.3, 80.7, 79.4, 70.9, 70.4, 70.4, 68.7, 61.4, 50.4, 46.0, 40.4, 34.6, 33.3, 28.6, 28.3, 20.3, 12.1; HRMS calcd. for $\text{C}_{32}\text{H}_{49}\text{N}_2\text{O}_{10}^+$: 621.3387; Found: 621.3379.

5-((7-((2-(2-(2-aminoethoxy)ethoxy)ethyl)(ethyl)amino)-2-oxo-2*H*-chromen-4-yl)methoxy)-5-oxopentanoic acid (7). As shown in **Scheme S1**, ester **6** (25 mg, 40.2 μmol , 1.0 equiv.) was dissolved in dichloromethane (0.7 mL) and treated with TFA (0.3 mL) at room temperature (23 °C). The reaction mixture was stirred for 1 h, and progress of the reaction was monitored by TLC. Upon completion, the reaction mixture was concentrated to dryness, and the excess TFA was removed azeotropically using toluene. The residue was re-dissolved in DMSO and purified by reverse phase chromatography using water and acetonitrile (both containing 0.1% TFA). Dissolution in water and lyophilization yielded pure **7** (18 mg, >95 % yield) as a viscous oil. ^1H NMR (400 MHz, Methanol- d_4) δ 7.49 (d, $J = 9.1$ Hz, 1H), 6.80 (dd, $J = 9.1, 2.6$ Hz, 1H), 6.69 (d, $J = 2.6$ Hz, 1H), 6.12 – 6.06 (m, 1H), 5.32 (d, $J = 1.3$ Hz, 2H), 3.98 (s, 1H), 3.75 – 3.61 (m, 11H), 3.55 (q, $J = 7.0$ Hz, 2H), 3.15 – 3.08 (m, 2H), 2.56 (t, $J = 7.4$ Hz, 2H), 2.39 (t, $J = 7.3$ Hz, 2H), 2.00 – 1.91 (m, 2H), 1.21 (t, $J = 7.0$ Hz, 3H); ^{13}C NMR (126 MHz, Methanol- d_4) δ 176.7, 175.5, 165.0, 158.7, 157.2, 152.6, 125.8, 110.6, 107.8, 105.2, 98.7, 71.8, 71.4, 70.6, 69.9, 60.8, 51.1, 46.6, 40.3, 36.1, 34.0, 22.3, 12.2; HRMS calcd. for $\text{C}_{23}\text{H}_{33}\text{N}_2\text{O}_8^+$: 465.2238; Found: 465.2231.

Photocleavage of PC linker. Photocleavage of 7- amino coumarin occurs from its meta carbon after excitation, which forms a tight ion pair (coumarinylmethyl cation and a leaving conjugate base) as key intermediates. The coumarinylmethyl cation reacts with a nucleophile resulting in bond cleavage and releasing the affinity-enriched

biomarker.²⁰ The PC linker was exposed to visible light (400–450 nm) and samples were taken at different time points (0, 1, 2, and 10 min total irradiation time). Photolysis products were monitored with UPLC (**Figure S1A**) and identified by mass spectrometry. The intact PC linker (**1**, 87%) concentration decreased with irradiation time and at 10 min, the chromatographic peak for the intact linker completely disappeared. Major photolysis product (**2**) was present in small amounts (5%) for the initial sample and that amount increased with the irradiation time up to 79%. In addition, UV-visible absorption (**Figure S1B**) and fluorescence measurements (**Figure S1C**) were used to monitor the photocleavage reaction. From the spectra shown in **Figure S1B**, very little changes in the absorption spectra were seen as a function of irradiation time. However, there was a slight increase in the fluorescence from the coumarin as a function of photocleavage of the starting material (**1**, **Figure S1C**). This may be due to an increase in the fluorescence quantum efficiency (ϕ) of the PC linker as a function of photocleavage from the meta carbon.

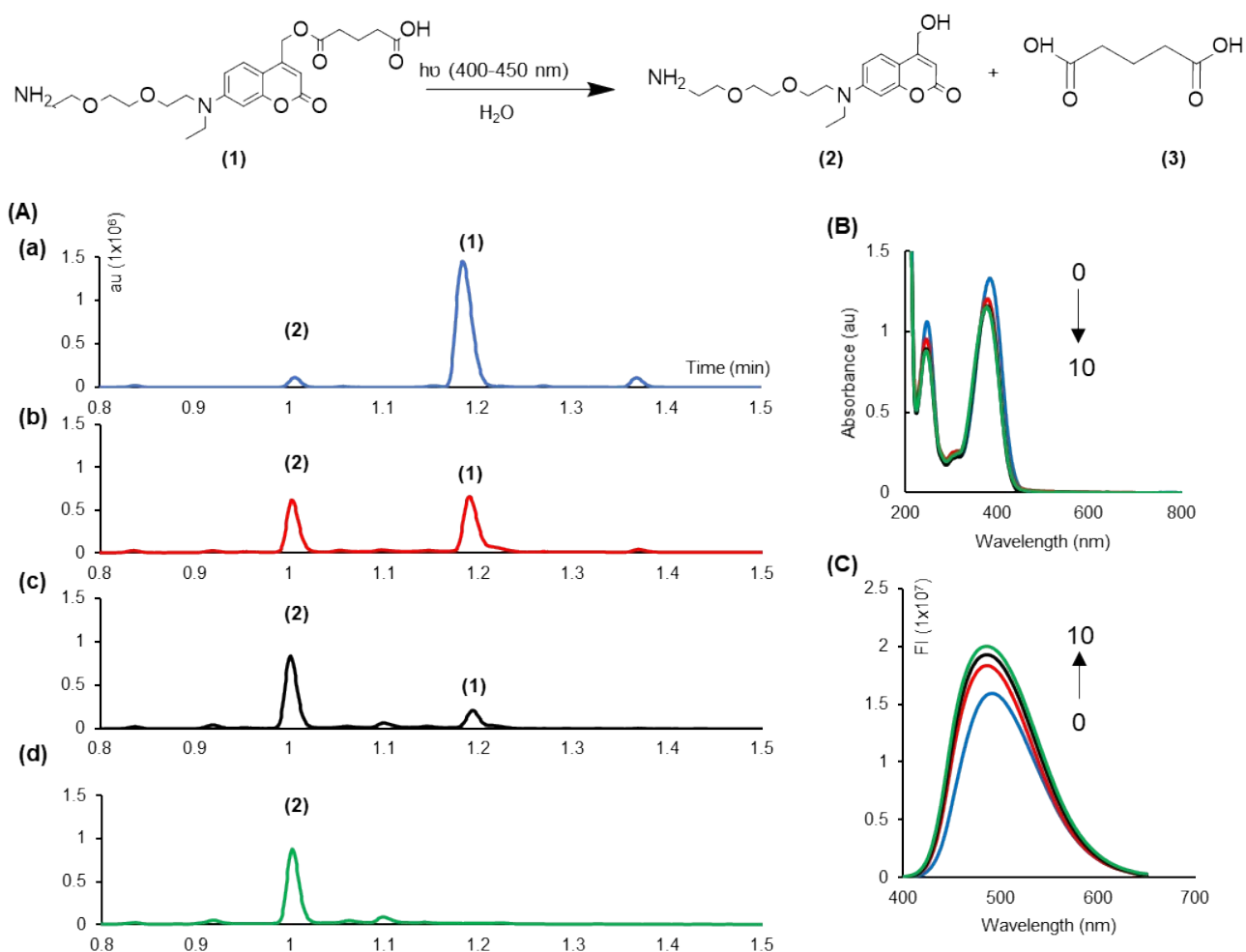


Figure S1. (A) Ultra-high performance liquid chromatography (UPLC) of the photocleavage of (1) using 400 – 450 nm light for exposure times of 0, 1, 2, and 10 min (a-d). The chromatography used a C18 column with an aqueous buffer and acetonitrile, ACN, as the mobile phase. (B) UV/vis spectra of the intact photolinker (1) as a function of exposure time. Same photo-irradiation conditions here as used in (A). (C) Fluorescence emission spectra of the photo-irradiated linker (1) as a function of time.

Stability of UV/O₃-activated COC in anhydrous solvents. COC is well-known for exceptional solvent resistance,¹ but the effect of anhydrous solvents on the stability of UV/O₃-activated COC has not been investigated. We tested planar COC surfaces – either unmodified or UV/O₃-activated – that were left in air, immersed in buffer (MES, pH 4.8), or immersed in anhydrous solvents – ACN or dimethylformamide (DMF) – for 2 h. Dichloromethane was also tested but was immediately rejected due to polymer swelling and degradation of the COC substrate upon exposure; no polymer degradation was observed for either ACN or DMF. After solvent exposure, the surfaces were rinsed with water, dried, and then evaluated by several surface analysis techniques (**Table S1**) including water contact angles (WCAs), -COOH densities via a colorimetric TBO assay, and ATR-FTIR spectroscopy.

Table S1. Surface analyses to evaluate the stability of UV/O₃-activated COC surfaces exposed to aqueous buffer or anhydrous solvents.

Surface treatment	WCA ^[f] (°)	-COOH ^[g] (nmol/cm ²)	ATR-FTIR (au / cm ⁻¹)	
			C=O ^[h]	O-H ^[i]
Unmodified ^[a]	94.2 ±4.7	0.2 ±0.1	0.2 ±0.1	0.0 ±0.3
Unmodified, MES	93.7 ±4.4	0.2 ±0.0	0.1 ±0.3	-0.1 ±0.4
Unmodified, DMF	86.6 ±7.6	0.1 ±0.0	0.1 ±0.3	0.0 ±0.5
Unmodified, ACN	90.6 ±5.6	0.3 ±0.1	-0.1 ±0.4	-0.2 ±0.7
UV/O ₃ ^[b]	36.5 ±2.5	1.8 ±0.3	5.6 ±0.0	3.3 ±0.4
UV/O ₃ , MES ^[c]	57.7 ±3.6	2.0 ±0.4	4.7 ±0.5	3.4 ±0.6
UV/O ₃ , DMF ^[d]	83.2 ±8.4	0.4 ±0.0	2.6 ±0.3	1.5 ±0.7
UV/O ₃ , ACN ^[e]	64.7 ±8.4	0.6 ±0.1	4.7 ±0.8	3.6 ±0.5

COC surfaces were [a] unmodified or [b] UV/O₃-activated and submersed in [c] MES (100 mM, pH 4.8), [d] DMF, or [e] ACN. [f] Water contact angles (WCA). [g] Carboxylic acid (-COOH). ATR-FTIR spectral features integrated from [h] 1650-1850 and [i] 3200-3700 cm⁻¹.

UV/O₃-activated COC surfaces not exposed to buffer or solvent, as expected, exhibited increased wettability and -COOH surface densities, which is supported by the appearance of carbonyl and hydroxyl peaks in the ATR-FTIR spectra. Treatment with MES buffer increased surface hydrophobicity and slightly decreased -COOH surface densities and ATR-FTIR peak areas. Based on previous studies, UV/O₃-activation produces a heterogenous surface containing different oxidized functionalities and scissioning of the polymer chains into smaller molecular weight fragments. While COC appeared to be more resistant to fragmentation than, for example PMMA, fragmentation is likely to occur to some extent.¹ We suspect that MES buffer immersion resulting in decreased oxidation signals may have been caused by solubilization of oxidized polymer fragments.

DMF treatment increased hydrophobicity appreciably and reduced -COOH densities to near the nonspecific limit of the TBO assay. Further, ATR-FTIR peak areas were reduced after DMF treatment compared to MES buffer. Along with the altered WCAs in the unmodified COC control, these data could indicate solvent penetration and partial solubilization of the surface even though no degradation or swelling of the bulk material was observed – only harsh solvents such as dichloromethane produced these artifacts for COC.

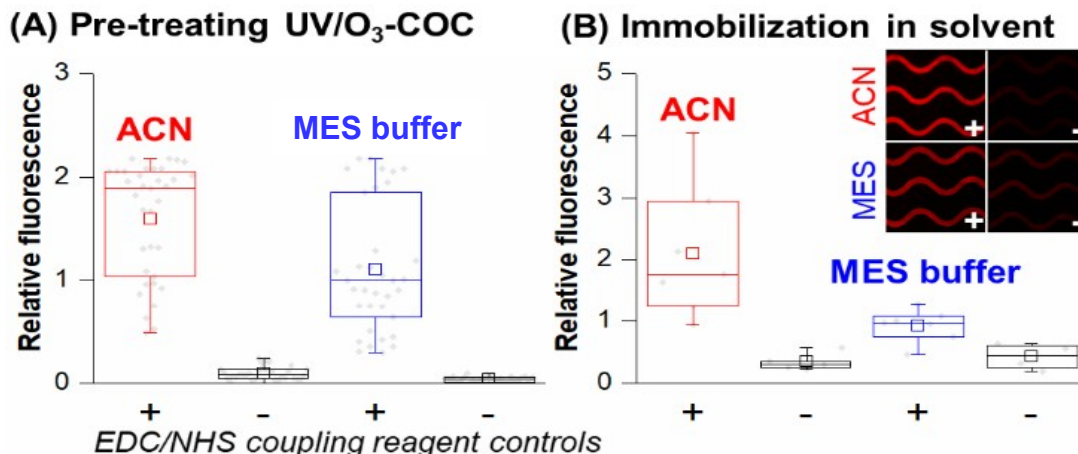


Figure S2. 5'-NH₂-, 3'-Cy5-oligonucleotide direct attachment to UV/O₃-COC surfaces. **(A)** ACN pre-treatment of UV/O₃-COC yielded similar loads of Cy5-oligonucleotides compared to MES (N = 33-35). **(B)** Improved Cy5 oligonucleotide loads were observed in fluorescence microscopy by EDC/NHS coupling in ACN (N = 4).

ACN treatment yielded a surface most comparable to the MES buffer treatment (**Figure S2**). The only concerning disparity between ACN and MES treatment was a 68% decrease in -COOH densities. The consequences for biomolecule immobilization are limited by the stoichiometric ratio of smaller -COOH groups and larger biomolecules. For example, a theoretical monolayer of -COOH groups is 830 pmol/cm², whereas a monolayer of larger oligonucleotides or antibodies is ~13 pmol/cm² or 0.85 pmol/cm², respectively. Thus, an approximate 3-fold decrease in -COOH densities as assessed by the TBO assay may be irrelevant for biomolecule immobilization (**Figure S2A**). High relative fluorescence intensities were observed when EDC/NHS reaction was conducted in ACN compared to MES buffer (**Figure S2B**). Dry ACN minimizes NHS ester hydrolysis and improves the efficiency of EDC/NHS coupling reaction. Based on these data, ACN solvent was selected for testing biomolecule coupling by EDC/NHS-activation.

LED exposure chamber for PC linker cleavage. We constructed a photo-exposure chamber using an LED outputting light from 385-470 nm ($\lambda_{\text{max}} = 412$ nm), which overlaps significantly with the PC linker's absorption spectrum (**Figure S3A**) and does not expose biological samples to intense UV radiation that may damage markers or their molecular cargo.^{15, 21} The LED was placed 24 mm from the device surface to allow the LED's innate divergence (60°) to provide a spot diameter of 90 mm, which provided relatively homogenous illumination over the CTC or EV enrichment device's surface area (34 ± 4 mW/cm²; **Figure S3B**). Lastly, we note that larger or smaller devices can be accommodated without any additional optical elements by simply changing the

distance between the LED light source and the device surface and elongating or shortening exposure time to achieve a consistent dose.

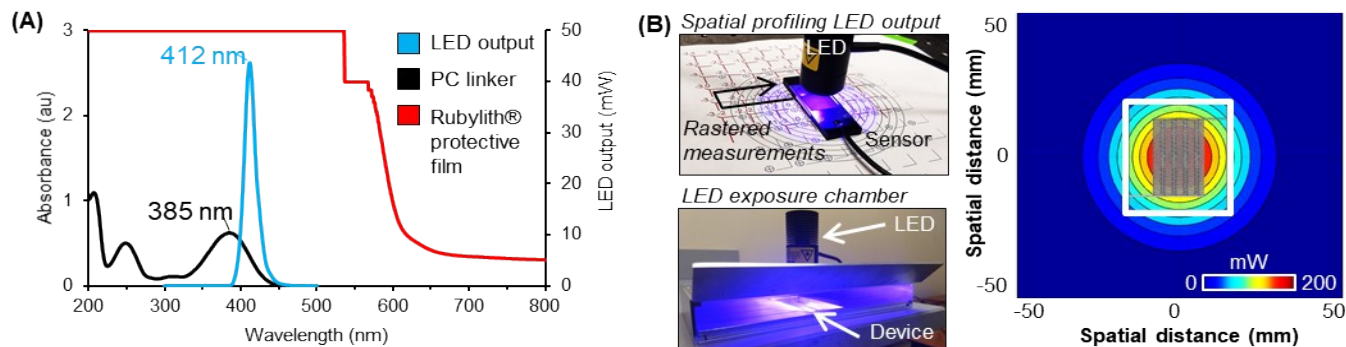
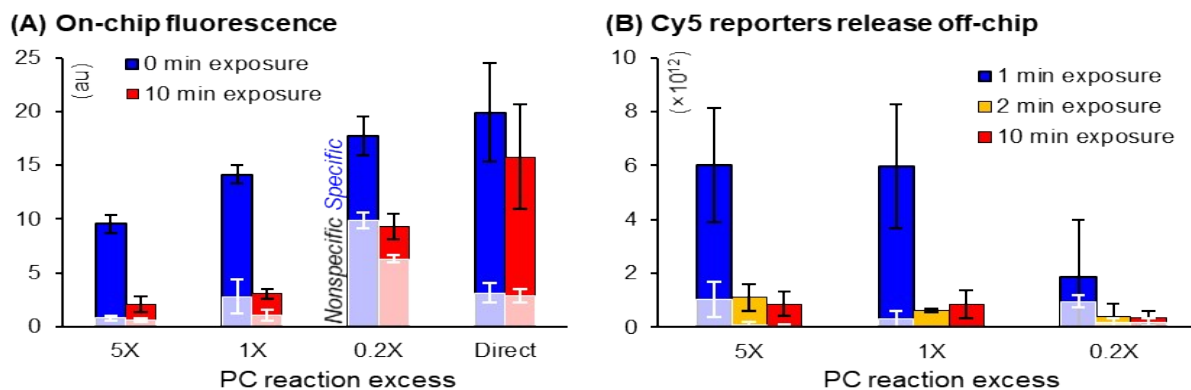


Figure S3. (A) The LED’s spectral output, the absorbance spectra of the PC linker (measured at 0.526 μM in PBS, pH 7.4), and the Rubylith® film used to protect devices from ambient light and premature photocleavage. **(B)** For photoexposure, the Rubylith® film is removed, and devices were inserted into an aluminum exposure chamber, where the LED was centered with a 90 mm spot size over the device (shown here is the sinusoidal CTC enrichment device – 26 mm \times 16 mm). The LED’s spatial flux was measured by rastering a sensor underneath the LED and fitting to a 2-dimensional Gaussian ($R^2 = 0.9986$), which showed uniform exposure ($34 \pm 4 \text{ mW/cm}^2$) over the device.

Cy5 reporter assay to monitor PC linker immobilization and cleavage. We immobilized the PC linker to UV/ O_3 -activated COC devices using ACN for the EDC/NHS reaction and triethylamine (TEA) organic base for PC linker conjugation to the formed NHS ester. Three concentrations of PC linker were tested for the immobilization reaction – 2.65 mM, 0.530 mM, and 0.106 mM – corresponding to reaction excesses of 5X, 1X, and 0.2X relative to a theoretical monolayer of PC linker (0.56 nmol/cm^2 , 1.82×10^{15} molecules per device). Before PC linker immobilization, the device was protected from ambient light by wrapping the device in Rubylith® film, which absorbs light throughout the PC linker’s absorption spectrum and protect the PC linker from photo cleaving

(Figure S3A).



Following selection of either CTCs or EVs, the film was removed before LED exposure.

Figure S4. The PC linker was immobilized at three concentrations with reaction excesses of 5X, 1X, and 0.2X relative to the sinusoidal microfluidic device's surface area and a theoretical monolayer of PC linkers. Immobilized PC linkers were labeled with a Cy5 oligonucleotide reporter by EDC/NHS conjugation, and the device was exposed to the LED for a total of 10 min to cleave the PC linker and release Cy5 reporters. **(A)** Fluorescence microscopy before and after 10 min LED exposure for positive and negative controls – negative controls lacked the EDC/NHS coupling reagents when immobilizing the Cy5 reporter. **(B)** The amount of Cy5 reporter molecules released after different exposure times, which were quantified by fluorescence microscopy. Note that the colored bars represent positive control data, and the overlaid, transparent white bars show data from negative controls, where the EDC/NHS coupling reagents were not included for the Cy5 oligonucleotide immobilization.

After immobilization, the PC linker was not visible by fluorescence microscopy using a DAPI filter set, most likely due to high autofluorescence of the UV/O₃-activated polymer at these wavelengths. Thus, we attached Cy5-labeled oligonucleotide reporter to the linker's -COOH group via EDC/NHS reaction (in ACN solvent). Fluorescence microscopy was used to visualize relative amounts of Cy5 reporter immobilized to the PC linker (**Figure S4A**).

On-chip Cy5 fluorescence signals were 8-11X higher than negative controls, where EDC/NHS coupling reagents were not included for Cy5 oligonucleotide immobilization.¹ Note that we observed an increase in nonspecific attachment as PC linker reaction excess decreased, even beyond nonspecific attachment to UV/O₃-COC alone (direct attachment, negative control). We suspect that the decreasing PC linker loads correspond to higher levels of Tris conjugated to the surface, altering the surface properties (namely H-bonding) and leading to increased nonspecific attachment of the oligonucleotide reporter. This hypothesis is further facilitated after we observed a high on-chip fluorescence in Tris treated devices compared to not treated devices (data not shown).

After attachment of the Cy5 oligonucleotide reporter and fluorescence microscopy interrogation, we used the LED exposure chamber to cleave the linker at various time points and release Cy5 oligonucleotide reporters that could subsequently be analyzed using fluorescence measurements (**Figure S4B**). These measurements validated that reductions in on-chip fluorescence (**Figure S4A**) corresponded to reporter release. They also provided direct quantitative data showing an equivalent load of reporters released with 1-5X PC linker reaction excess but a sharp reduction in reporter immobilized at 0.2X excess. Note that we quantified the effects of photobleaching in the direct immobilization control, where Cy5-labeled oligonucleotide reporter was immobilized to the surface directly without involving the PC linker. It showed a ~20 % loss in Cy5 fluorescence after LED exposure. In separate experiments, we confirmed photobleaching occurred during fluorescence microscopy imaging (Cy5 channel), but not during LED photoexposure (data not shown). This was not unexpected as the LED output (385-470 nm) is well separated from the absorbance range of the Cy5 fluorophore (507-694 nm, $\lambda_{max} = 649$ nm).

Flow cytometry analysis of antigen expression in cell lines and correlation to release efficiency. For the affinity-enriched cell lines, we analyzed antigen expression versus isotype controls by flow cytometry (**Figure S5A**). MCF7 had the highest expression of EpCAM (125X IgG) with lower expression of EpCAM in the SKBR3 cell line (20X). For enrichment anti-EpCAM antibodies were used for enriching MCF7 and SKBR3 cell lines, while

anti-FAP α antibodies were used for enriching the Hs578T cells. Release efficiencies were 88 \pm 10%, 94 \pm 4%, and 91 \pm 4% for the MCF7, SKBR3, and Hs578T cell lines, respectively. We observed minimal correlation between antigen expression and release efficiency (**Figure S5B**). Therefore, the rate of release does not seem to depend on the number of Ab-antigen interactions. We previously encountered results which indicated that when using the enzymatically cleavable oligonucleotide linker,²² longer incubation times with USER enzyme were required to achieve equivalent release efficiency for cells with higher antigen expression levels.¹³

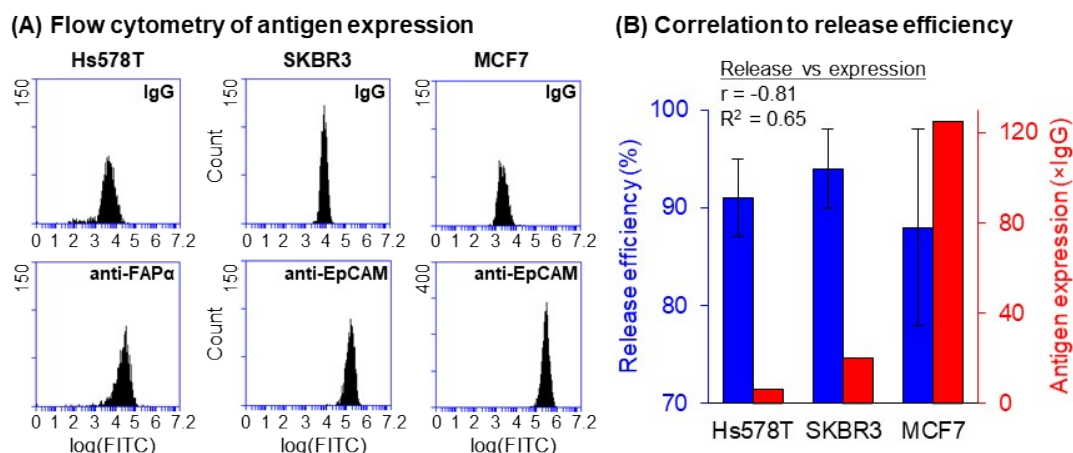


Figure S5. (A) Three cell lines (Hs578T, SKBR3, and MCF7) were tested for antigen expression by flow cytometry. Cells were labeled with FITC-conjugated IgG control Abs and their corresponding FITC-labeled primary Ab, anti-FAP α or anti-EpCAM. Labeled cells were analyzed with a BD Accuri C6 Plus flow cytometer. **(B)** Relative antigen expressions were obtained by flow cytometry data and correlated ($r = -0.81$) with release efficiency.

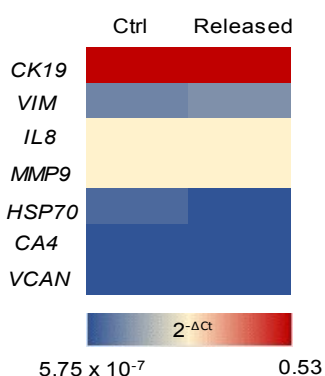
Impact of RNA 8-oxo-G damage on gene expression. Total RNA was purified from Hs578T cells from standard culture (control) or after LED exposure (18.5 J), or after UV exposure (18.5 J) or after H₂O₂ treatment. mRNA was reverse transcribed with anchored poly(dT) primers and cDNA was amplified with gene specific primers (**Table S2**) by qPCR with 2-3 replicates per gene. All genes were referenced to the housekeeping gene *GAPDH* and reported as $2^{-\Delta C_t}$, where ΔC_t is $C_t^{\text{Gene}} - C_t^{\text{GAPDH}}$. No interfering amplification was observed in RT controls for all genes and samples (data not shown).

Table S2. Gene-specific primers for evaluating Hs578T and SKBR3 gene expression by RT-qPCR.

Gene/cDNA	Forward 5'-3'	Reverse 5'-3'	Product size (bp)
<i>Vim</i>	AAT CTT GTG CTA GAA TAC TTT	TTT CCA AAG ATT TAT TGA AGC	112
<i>CD44</i>	ATT AAA CCC TGG ATC AGT C	TCG AAG AAG TAC AGA TAT TTA TTA T	107
<i>CK19</i>	CTT CTG CTG TCC TTT GG	CCC TTG GAC CAT AAA TTT TTA	108
<i>MMP9</i>	ACC GAG AGA AAG CCT ATT	GGG ATT TAC ATG GCA CTG	162
<i>SMA</i>	CAT TGT CCA CAG GAA GT	TAA GGC TTG TAG GTT TTA ATG	103
<i>FAP v2</i>	AAG GGA GTC ATG CAT TT	TAG CAC TTG AAC TTC TGA	87
<i>IL8</i>	TGA TAC TCC CAG TCT TGT C	AAG TTT CAA CCA GCA AGA A	131

<i>HSP70</i>	AGG TGA AAG CAA TGT TAA AG	CTT CCC AGG ATA ACT GAA G	122
<i>CA4</i>	AGC GCA CGG TGA TAA A	GAA GCC TGG AAC TTG GA	164
<i>VCAN</i>	AGA GCC ACA GAGCAT TT	TCT CAA AGA AAC AGA GTG ATA	156
<i>GAPDH</i>	TGG TTG AGC ACA GGG TA	TCA CAG TTG CCA TGT AGA C	93

Impact of remaining Ab ligand on gene expression. Molecular level changes due to the attachment of Ab on cell surface and photo-release were evaluated by profiling mRNA expression of photo released cells. Total RNA was extracted and RT reaction were performed. QPCR was performed with selected genes including “stress genes” (Table S2 for primer sequences). mRNA expression profiles are shown in Figure S6. Data were normalized to the house keeping gene *GADPH* as mentioned above. We observed similar mRNA expression profiles in photo-released cells and control cells ($p > 0.05$, Pearson coefficient = 0.99). The results suggest that, monoclonal Ab attachment on cell surface (i.e., as a ligand) did not alter the mRNA expression of target genes



within 1-2 h of sample processing under these experimental conditions.

Figure S6. RT-qPCR was used to analyze mRNA expression changes occurred due to the presence of Ab ligands on cell surface after photo release. mRNA expression profiles of 7 genes were with control SKBR3 cells and photo released cells. Cell isolation experiments were performed in duplicate and gene expression analysis was tested 5, 6 times. (For *CK19*, N=5 and for other genes N=6). The gene panel consists of stress genes, epithelial and mesenchymal markers.

RT-ddPCR of MOLT-3 EV-mRNA after LED exposure. EVs from MOLT-3 cells were PEG precipitated, resuspended in PBS, and exposed to LED irradiation for 2 min or not (control). Afterwards, the EVs were lysed via Trizol, and EV-RNA was extracted and quantified. We probed a panel of 8 genes by RT-ddPCR (primer sequences in Table S3). We did not observe any effect of LED exposure on RT-ddPCR results for this EV-mRNA panel (see Figure S7).

Table S3. Gene-specific primers for MOLT-3 EV-mRNA profiling by RT-ddPCR.

Gene/cDNA	Forward 5'-3'	Reverse 5'-3'	Product size (bp)
<i>PLBD1</i>	GTA CTG AGA TGC TAG GTA GAT A	CAA GGG AAA GTG ACT GAT AC	189
<i>FOS</i>	TGC CAG GAA CAC AGT AG	TTC AGA GAG CTG GTA GTT AG	188

<i>MMP9</i>	GGG ATT TAC ATG GCA CTG	ACC GAG AGA AAG CCT ATT	162
<i>CA4</i>	GAA GCC TGG AAC TTG GA	AGC GCA CGG TGA TAA A	164
<i>VCAN</i>	TCT CAA AGA AAC AGA GTG ATA	AGA GCC ACA GAGCAT TT	156
<i>IL8</i>	AAG TTT CAA CCA GCA AGA A	TGA TAC TCC CAG TCT TGT C	131
<i>CD8a</i>	GCC ACT CAT AAC AGC ATA G	TGC CCA TTG GAG AGA AA	178
<i>CD81</i>	GGA GGG AAC AAG GTG AG	TGT AGG TGG CGT GTA TG	210

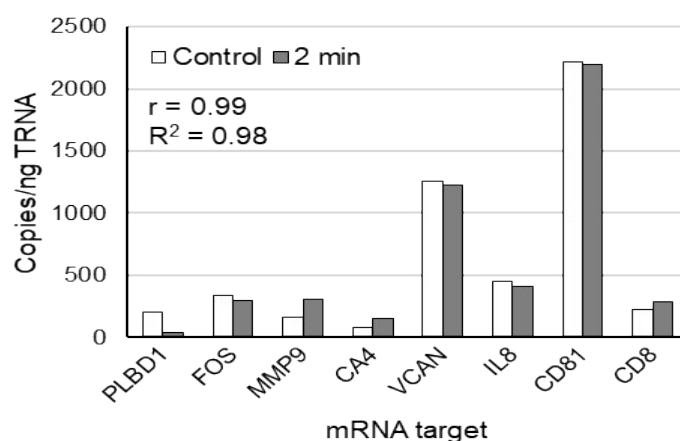


Figure S7. RT-ddPCR results for 8 genes from MOLT-3 EVs irradiated with LED light for 2 min (18.5 Joule dose) compared to non-irradiated EVs. Very strong correlation was observed between the two data sets, indicating that RNA oxidation (observed in **Figure 3F** of the main manuscript) does not affect the ability to perform RT-ddPCR from EV-RNA in this gene panel. PLBD1, FOS, MMP9, CA4, and VCAN are genes whose activity is dysregulated as a result of an AIS event. IL8 is a stress gene, CD81 is a gene that transcribes the exosome-specific tetraspanin, and CD8 is the selection antigen for EVs related to AIS.

Short Tandem Repeat (STR) data of cell lines

Table S4. Short Tandem Repeat (STR) identification information of all the cell lines used in this manuscript. The data were extracted from American Type Culture Collection (ATCC) STR data base.

% Match	ATCC Number	Designation	D5S818	D13S317	D7S820	D16S539	vWA	TH01	AMEL	TPOX	CSF1PO
100	HTB-30	SK-BR-3Breast Adenocarcinoma Human	9,12	11,12	9,12	9	17	8,9	X	8,11	12
100	HTB-126	Hs 578TBreast Carcinoma Human	11	11	10	9,12	17	9,9.3	X	8	13
100	HTB-22	MCF7Breast Adenocarcinoma Human	11,12	11	8,9	11,12	14,15	6	X	9,12	10
100	CRL-1552	MOLT-3 Leukemia; Human	12	12,13	8,10	11,13,14	17	6,8	X,Y	8	11,12

All cell lines used in this manuscript were purchased from ATCC and STR identification was conducted by the supplier.

Supplementary References

1. J. M. Jackson, M. A. Witek, M. L. Hupert, C. Brady, S. Pullagurla, J. Kamande, R. D. Aufforth, C. J. Tignanelli, R. J. Torphy, J. J. Yeh and S. A. Soper, *Lab Chip*, 2014, **14**, 106-117.
2. A. A. Adams, P. I. Okagbare, J. Feng, M. L. Hupert, D. Patterson, J. Gottert, R. L. McCarley, D. Nikitopoulos, M. C. Murphy and S. A. Soper, *J. Am. Chem. Soc.*, 2008, **130**, 8633-8641.
3. U. Dharmasiri, A. A. Adams, M. Witek and S. A. Soper, *Annu. Rev. Anal. Chem.*, 2010, **3**, 409-431.
4. U. Dharmasiri, S. Balamurugan, A. A. Adams, P. I. Okagbare, A. Obubuafo and S. A. Soper, *Electrophoresis*, 2009, **30**, 3289-3300.
5. U. Dharmasiri, S. K. Njoroge, M. Witek, M. G. Adebisi, J. W. Kamande, M. L. Hupert, F. Barany and S. A. Soper, *Anal. Chem.*, 2011, **83**, 2301-2309.
6. M. L. Hupert, J. M. Jackson, H. Wang, M. A. Witek, J. Kamande, M. I. Milowsky, Y. E. Whang and S. A. Soper, *Microsys. Technol.*, 2014, **20**, 1815-1825.
7. J. M. Jackson, J. B. Taylor, M. A. Witek, S. A. Hunsucker, J. P. Waugh, Y. Fedoriw, T. C. Shea, S. A. Soper and P. M. Armistead, *Analyst*, 2016, **141**, 640-651.
8. J. W. Kamande, M. L. Hupert, M. A. Witek, H. Wang, R. J. Torphy, U. Dharmasiri, S. K. Njoroge, J. M. Jackson, R. D. Aufforth, A. Snavely, J. J. Yeh and S. A. Soper, *Anal. Chem.*, 2013, **85**, 9092-9100.
9. M. A. Witek, R. D. Aufforth, H. Wang, J. W. Kamande, J. M. Jackson, S. R. Pullagurla, M. L. Hupert, J. Usary, W. Z. Wysham, D. Hilliard, S. Montgomery, V. Bae-Jump, L. A. Carey, P. A. Gehrig, M. I. Milowsky, C. M. Perou, J. T. Soper, Y. E. Whang, J. J. Yeh, G. Martin and S. A. Soper, *NPJ Precis. Oncol.*, 2017, **1**, 24.
10. C. D. Campos, S. S. Gamage, J. M. Jackson, M. A. Witek, D. S. Park, M. C. Murphy, A. K. Godwin and S. A. Soper, *Lab Chip*, 2018, **18**, 3459-3470.
11. C. E. O'Neil, J. M. Jackson, S. H. Shim and S. A. Soper, *Analytical Chemistry*, 2016, **88**, 3686-3696.
12. C. E. O'Neil, S. Taylor, K. Ratnayake, S. Pullagurla, V. Singh and S. A. Soper, *Analyst*, 2016, **141**, 6521-6532.
13. S. V. Nair, M. A. Witek, J. M. Jackson, M. A. Lindell, S. A. Hunsucker, T. Sapp, C. E. Perry, M. L. Hupert, V. Bae-Jump, P. A. Gehrig, W. Z. Wysham, P. M. Armistead, P. Voorhees and S. A. Soper, *Chem. Commun.*, 2015, **51**, 3266-3269.
14. T. M. Runger and U. P. Kappes, *Photodermatol. Photoimmunol. Photomed.*, 2008, **24**, 2-10.
15. E. Sage, P. M. Girard and S. Francesconi, *Photochem. Photobiol. Sci.*, 2012, **11**, 74-80.
16. S. G. Nyaga, A. Lohani, P. Jaruga, A. R. Trzeciak, M. Dizdaroglu and M. K. Evans, *BMC Cancer*, 2006, **6**, 297.
17. M. G. Adamski, Y. Li, E. Wagner, C. Seales-Bailey, N. Bennett, H. Yu, M. Murphy, S. A. Soper and A. E. Baird, *Med. Res. Arch.*, 2017, **5**.
18. M. A. Rider, S. N. Hurwitz and D. G. Meckes, Jr., *Sci. Rep.*, 2016, **6**, 23978.
19. C. Bao, G. Fan, Q. Lin, B. Li, S. Cheng, Q. Huang and L. Zhu, *Org. Lett.*, 2012, **14**, 572-575.
20. P. Klan, T. Solomek, C. G. Bochet, A. Blanc, R. Givens, M. Rubina, V. Popik, A. Kostikov and J. Wirz, *Chem Rev*, 2013, **113**, 119-191.
21. J. M. Jackson, M. A. Witek, J. W. Kamande and S. A. Soper, *Chem. Soc. Rev.*, 2017, **46**, 4245-4280.

22. S. V. Nair, M. A. Witek, J. M. Jackson, M. A. M. Lindell, S. A. Hunsucker, T. Sapp, C. E. Perry, M. L. Hupert, V. Bae-Jump, P. A. Gehrig, W. Z. Wysham, P. M. Armistead, P. Voorhees and S. A. Soper, *Chemical Communications*, 2015, **51**, 3266-3269.